SAM-TDR-64-23

THORACIC CAGE IMPEDANCE MEASUREMENTS

Impedance Plethysmographic Determination of Cardiac Output (An Interpretive Study)

TECHNICAL DOCUMENTARY REPORT NO. SAM-TDR-64-23

May 1964

USAF School of Aerospace Medicine
Aerospace Medical Division (AFSC)
Brooks Air Force Base, Texas

Task No. 775801

(Prepared under Contract No. AF 41(657)-403 with the University of Minnesota, Minneapolis, Minnesota)

FOREWORD

This report was prepared in the Departments of Electrical Engineering and Physical Medicine, University of Minnesota, Minneapolis, Minnesota, by—

EDWIN KINNEN, Ph.D.
WILLIAM KUBICEK, Ph.D.
D. WITSOE, B.S.

ABSTRACT

The current flux distribution in the human thorax between band electrodes placed at the base of the neck and around the lower thorax, using 100 kc. excitation, was investigated to explain known correlations between the thorax electrical impedance waveforms and cardiac activity—particularly cardiac output.

Measurements of the current densities around the band electrodes, equipotential surfaces constructed from both surface and interior potential measurements, externally observed directed flux impedance waveforms, and impedance properties of an approximate thorax model indicated that the major portion of electrode current flux passed through the lung tissues rather than through the blood volumes of the heart having lower resistivity. The impedance plethysmographic waveforms, obtained between the band electrodes, therefore appeared to monitor the right ventricular stroke volume as reflected by impedance changes in the pulmonary vascular bed.

This technical documentary report has been reviewed and is approved.

Harold V. Ellingson

HAROLD V. ELLINGSON
Colonel, USAF, MC
Commander

THORACIC CAGE IMPEDANCE MEASUREMENTS

Impedance Plethysmographic Determination of Cardiac Output

(An Interpretive Study)

1. INTRODUCTION

Applications of impedance plethysmography to problems of monitoring physiologic activity in human thorax have been extended in an attempt to establish a procedure for measuring cardiac output. The procedure is based on the measurement of electrical impedance changes at 100 kc. between a set of electrodes which are placed on the surface of the thorax with minimum subject preparation and constraint. Although a variety of electrodes have been investigated for potential use, results obtained with two braided band electrodes, one around the neck and the other around the subject's midsection (fig. 1), have shown the most promise for further development. By limited comparisons with oxygen consumption rates, experimentally determined values of cardiac output, obtained from these impedance measurements have been found to be significantly correlated to reported results with the Fick, dye dilution, and Grollman procedures (1). The procedure has also been shown to be relatively insensitive to body type and lung air volume.

Any attempt to calibrate or even justify the determination of cardiac output from impedance measurements must be based on an understanding of the physiologic phenomena responsible for the measured variations. This implies that the exciting current flux paths in the thorax between the two band electrodes must be established. This report presents two hypotheses concerning the current flux distribution in the thorax and the results of an investigation carried out to examine these hypotheses.

A recent study of the average resistivity properties of thoracic tissue at 100 kc. has determined that lung tissue, skeletal muscle, heart muscle, and whole blood have approximate values of 1,200, 400, 450, and 155 ohm cm., respectively (2). For the band electrode and for recognizing the significant difference of resistivity and cross-section area between the lung tissue and the whole-blood volumes, two possible flux distributions of the exciting current in the human thorax are suggested:

1. Most of the current flux passes between the band electrodes through the lower resistivity volumes of the major thoracic arteries and veins and the heart; in general, it avoids the higher resistivity lung volumes. The implication of this hypothesis is that the band impedance waveform represents the changing dimensions of the major blood volumes of the thorax.

2. Most of the current flux passes from the band electrodes into the lung volume and tends to avoid the blood-volume regions. It has been determined that the magnitude and waveform of the impedance measured across the band electrodes are essentially independent of lung air volume (1). Consequently, the hypothesis of alternate current flux distribution implies that the measured impedance is an indication of the total movement of blood in the pulmonary vascular bed. While the measured impedance and observed waveform may not be predominantly attributable to either hypothesis, it is unlikely, in view of the results reported here, that they are equally attributable to both hypotheses.

2. SUMMARY

The results may be summarized as follows:

1. The impedance waveforms resulting from the use of two band electrodes appeared to reflect the arterial blood pulsations in the lungs and arteries

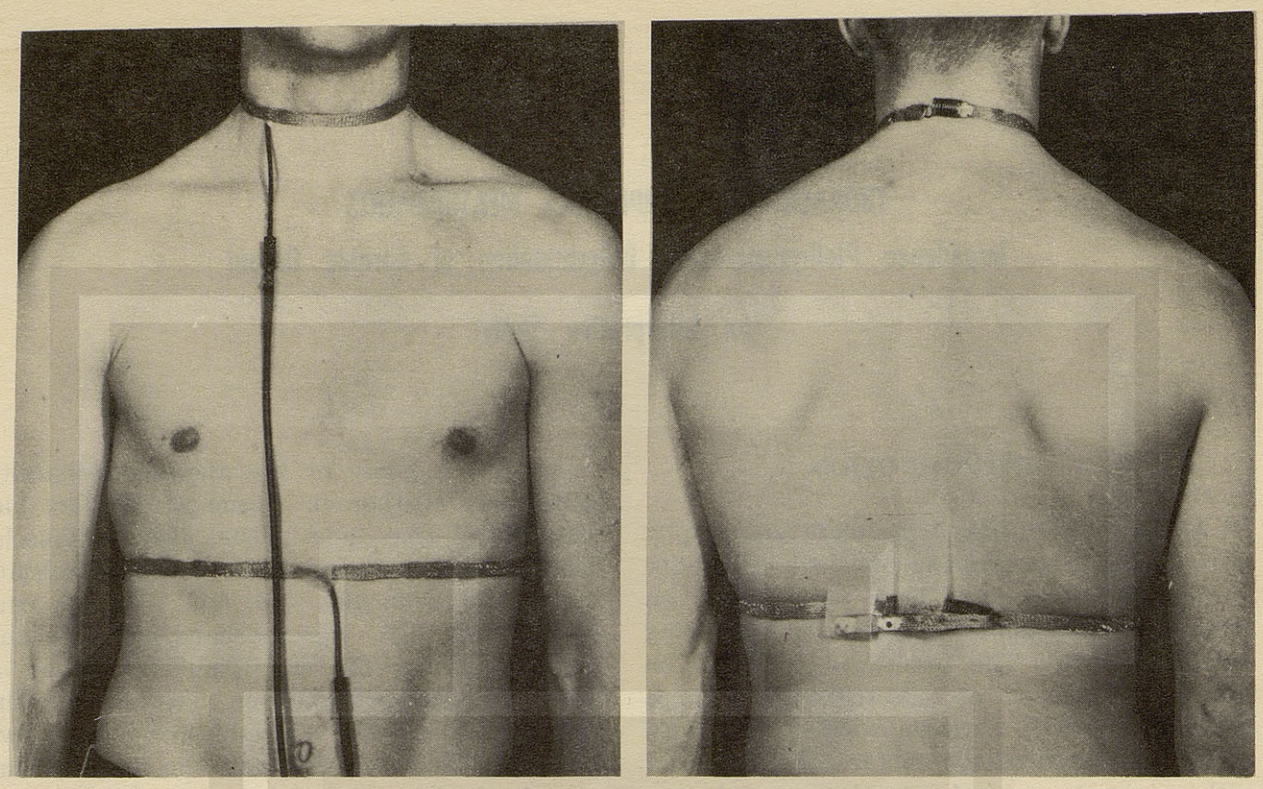

FIGURE 1

Two band electrodes positioned for recording changes in thoracic impedance.

rather than the ventricular volume; directed field waveforms indicated lower resistance of flux paths in volume regions of decreasing impedance during systole.

2. The equipotential surfaces sketched from potential measurements of the thorax indicated a flow of current from the blood-volume regions.

3. The largest density of the current leaving the midsection band electrode was found at the base of the lungs on the posterior thorax.

4. An approximate model of the thorax showed that most of the current passed through the model volume represented by lung tissue.

Each of these results would indicate that most of the current flux using the two band electrodes passed through the lungs so that the major impedance characteristics observed were controlled by the pulsating pulmonary arterial blood flow. Furthermore, the relatively accurate determinations of the cardiac output made from these impedance measurements were apparently based on an indirect indication of right ventricular stroke volume as reflected by the pulmonary vascular bed.

3. METHOD

The determination of the distribution of the internal current flux, corresponding to the band electrodes shown in figure 1, was developed from: (a) the analysis of the impedance waveforms obtained at various surface and internal locations of the thorax; (b) a direct measurement of voltage potentials on and in the thoracic volume; (c) an examination of current density through the electrode skin surface; and (d) a study of a simplified three-dimensional model of the thorax.

Impedance waveforms were obtained across two electrodes with a General Radio impedance comparator, model 1605A, and from three

electrodes coupled to an impedance plethysmograph. The comparator functioned as a signal source and as an electrical bridge, with an output voltage representation of the bridge imbalance around a null (1). The impedance plethysmograph was constructed from a constant current source and a high-impedance probe system capable of measuring impedance (potential) variations with respect to either of the source electrodes. A block diagram of this plethysmograph is given in figure 2. For the two band electrodes shown in figure 1, and for the 100-kc. excitation frequency, used throughout this investigation (2), the thorax presented an average impedance of $37 \times 10^{-3} \times \epsilon^{i\ 15^\circ}$ mhos/cm.^{2} The band electrodes were made from tinned copper braid shielding, 336 x 34 stranding. The braid was stretched to a width of about 1 cm. and coated on the inner side with Translyte electrode paste to provide a low-impedance skin contact. The electrodes were applied approximately 5 minutes before data were taken to allow the skin and paste to reach an equilibrium.

Five probe configurations were used in conjunction with the impedance plethysmograph to measure potential points on the surface and at various internal points of the thorax of human subjects and dogs. The external thorax surface probe was the ¾-in. circular brass disc, shown in edge view at the left of *A* in figure 3. The probe used for potential measurements in the human esophagus was machined from stainless steel and attached to a nasogastric tube (see *B* in fig. 3). A probe similar to the human esophagus probe, but of larger dimension (*C* in fig. 2), was used for

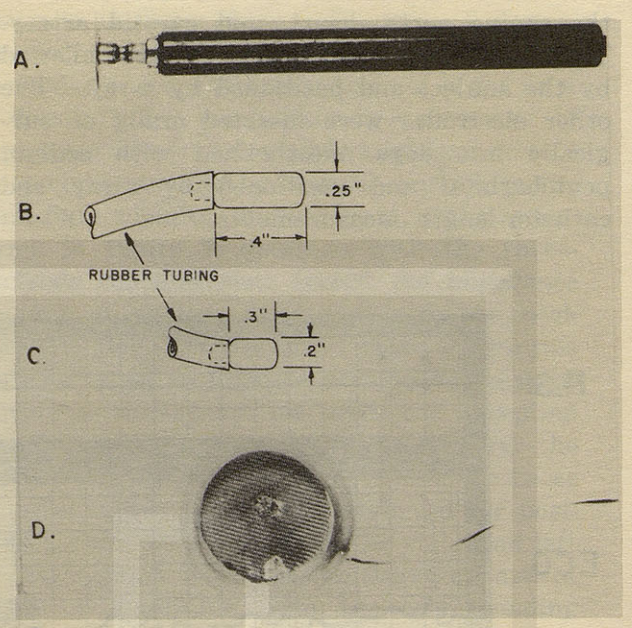

FIGURE 3

Surface and internal electrode configurations: **A**, *surface disk and insulated shank;* **B**, *human esophagus;* **C**, *canine trachea;* **D**, *surface cup electrode with stainless steel wire mesh.*

measuring potentials in the trachea and large bronchi of dogs. To obtain measurements in the lower esophagus, a canine esophagus electrode was constructed with the metal contact from the lung probe mounted at the end of a ¼-in. rigid Plexiglas tube. A 0.003-in. stainless steel wire inserted in a saline-irrigated catheter was used to determine potentials in

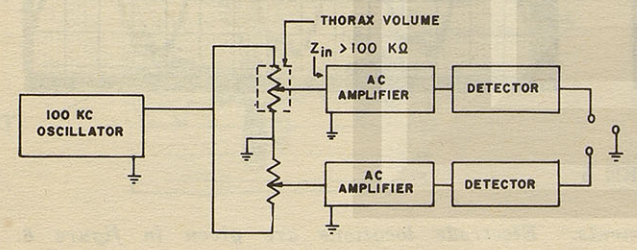

FIGURE 2

Block diagram of the impedance plethysmograph.

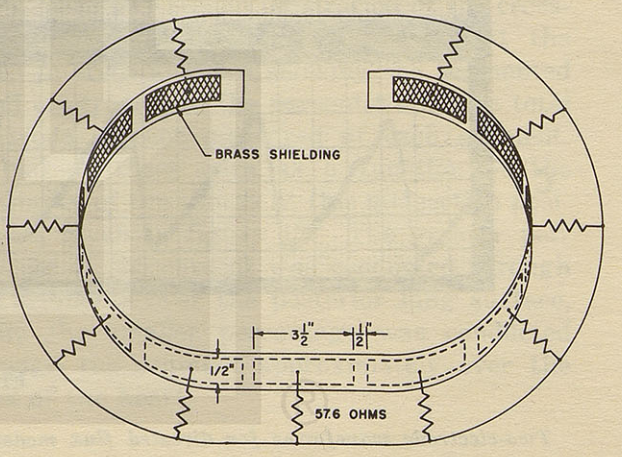

FIGURE 4

Segmented midsection band electrode.

the canine aorta, heart, and carotid artery. The human esophagus electrode was swallowed by the subject and positioned by x-ray. The other electrodes were inserted orally or surgically into dogs anesthetized with sodium pentobarbital and positioned by x-ray and catheter-length measurements.

The current distribution around the midsection electrode was measured with a segmented band electrode to which precision resistors were attached (fig. 4). Shielding braid provided the segmented material. When this electrode and the neck electrode were excited by a 100-kc. constant current source,

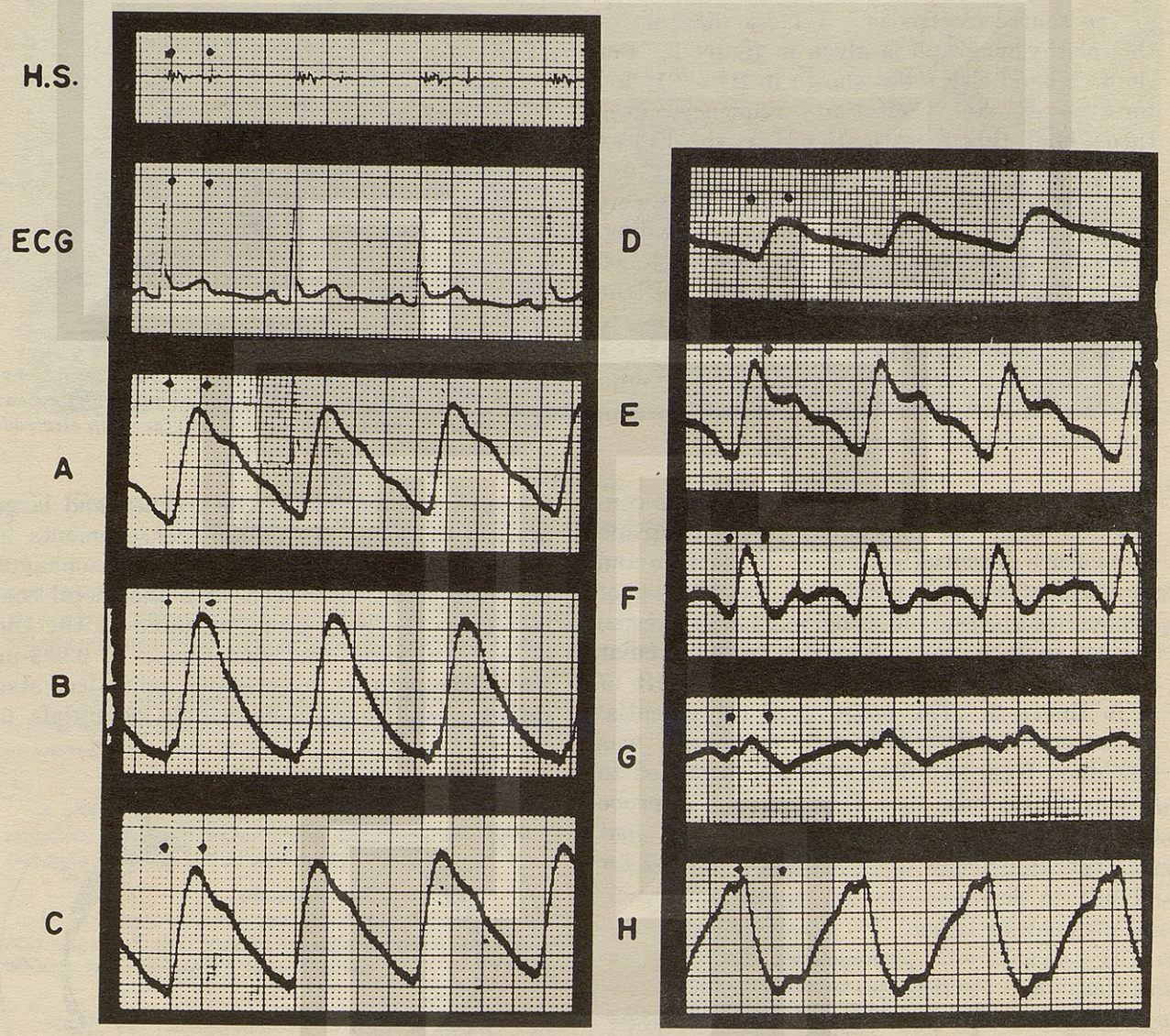

FIGURE 5

Two-electrode waveforms for directed flux measurements. Electrode locations are given in figure 6. **A**, *n to m;* **B**, *n to 2 posterior;* **C**, *n to 7 posterior;* **D**, *3 posterior to 4 posterior;* **E**, *n to 5 anterior;* **F**, *n to 6 anterior,* **G**, *7 anterior to 7 posterior;* **H**, *1 anterior to 7 anterior. Impedance decreasing upward.*

Subject: male, 71 in., 191 lb., sitting.

the root mean square voltage drop, noted across each resistor, was an indication of the thoracic current at that portion of the band surface.

To determine the possible contribution of various portions of the thorax to the impedance waveform observed between the neck and midsection electrodes, the 2-in. circular cup electrode filled with Redux electrode paste (shown in *D* of fig. 2) was used with a second similar electrode, or with the neck electrode, to provide directed flux waveforms. Coupled to the impedance comparator, this electrode was positioned over a volume region to direct the current and thereby localize the waveform to various portions of the thorax. By this procedure, dynamic impedance characteristics of the smaller volumes could be investigated and compared with the dominant characteristics of the two band waveforms.

4. RESULTS

The results of the investigation are as follows:

1. Typical impedance waveforms corresponding to directed flux measurements are presented in figure 5 for the corresponding electrode locations given in figure 6. A typical waveform obtained while using the two band electrodes (neck and midsection) is given in *A* of figure 5 for comparison. A decrease of impedance is noted for each waveform except those corresponding to thoracic regions in the immediate vicinity of the heart. The waveforms in figure 7, obtained with the three-electrode configuration, record the impedance changes at various distances from the neck electrode along the sternum. These waveforms are also noted to indicate a rapid decrease of impedance during systole, with the exception of *G* in figure 7—a position localized over the heart. Impedance waveforms similar to those given in figure 7 were also observed for positions approximately 5 cm. to the right and left of the sternum with no significant change of shape or amplitude from the corresponding waveforms noted directly over the sternum.

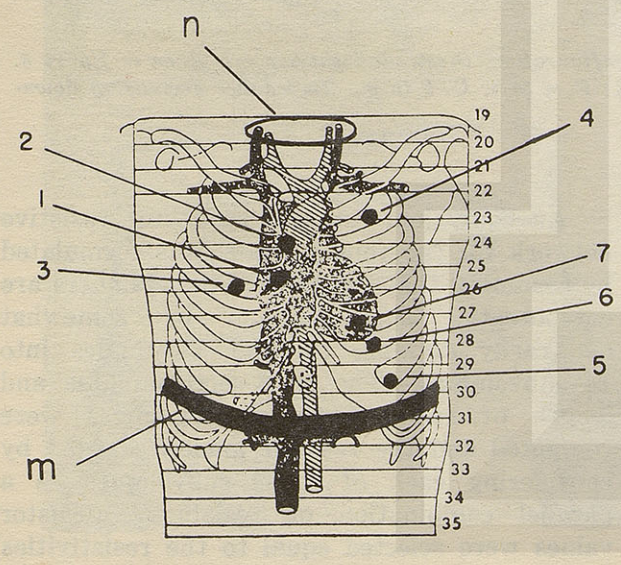

FIGURE 6

Surface electrode locations for waveforms in figure 5.

2. Equipotential voltages were determined on the surface of the thorax and in the esophagus of a young male subject. The results of this investigation are given in figures 9 and 10. The equipotential lines in figure 10 were sketched from the surface potentials shown in figure 9. Following similar potential measurements on the surface and in the esophagus, aorta, heart, carotid artery, trachea, and large bronchi of an anesthetized dog, the estimated potential surfaces of the animal thorax were also drawn (fig. 11).

3. Figure 12 is an illustration of the cross-sectional view of the human thorax at the third intercostal space showing the segmented band electrode and the percentage of the total electrode current measured at each segment. A plot of these data as a function of the perimeter of the thorax at this midsection position is given in figure 13. The greater percentage of the current was conducted through the segments over the posterior lung surface, while the smaller percentage was conducted through the segment approximately over the apex of the heart.

4. A simple model was constructed of the human thorax representing only the lung tissue volume, heart blood volume, and an upper

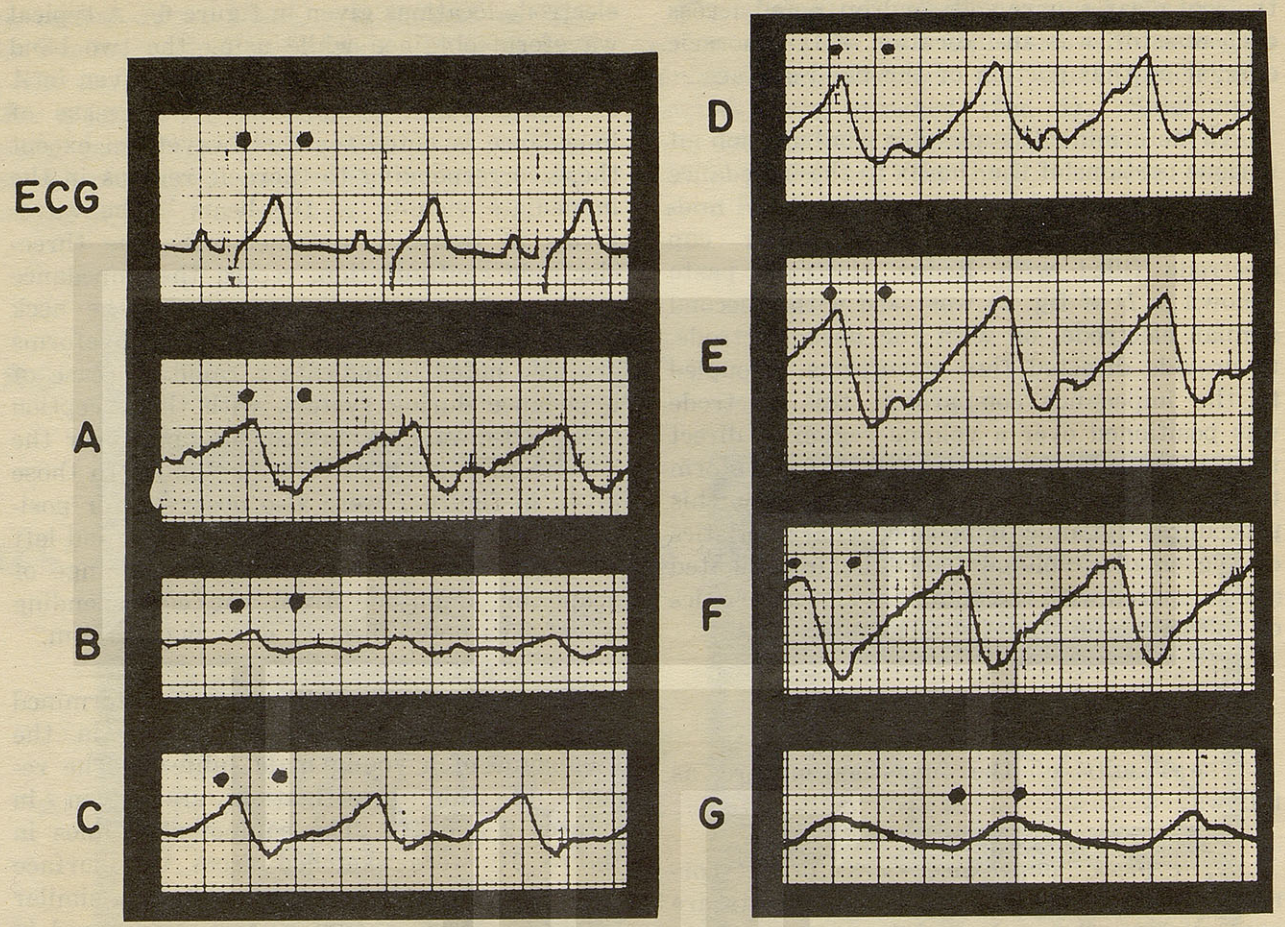

FIGURE 7

Three-electrode waveforms for band electrode flux configuration. Electrode locations are given in figure 8. **A**, *n to m;* **B**, *n to 1;* **C**, *n to 2;* **D**, *n to 3;* **E**; *n to 4;* **F**, *n to 5;* **G**, *5 to m. Impedance decreasing downward.*

Subject: male, 73 in., 170 lb., sitting.

thoracic blood volume corresponding to the major veins and arteries (fig. 14). Cylindric shapes were chosen to facilitate analysis and then divided into quadrants, as shown. To establish resistance values corresponding to the components of this model, average resistivities of lung tissue and blood were taken to be 1,200 ohm cm. and 155 ohm cm., respectively (2). Representative volumes of 5,000 cc. and 540 cc. were used to establish the dimensions of the lung volume and heart blood volume at the beginning of systole. The inner cylinder above the model heart cylinder was based on an upper thoracic major vein and artery volume of 60 cc.

An equivalent lumped parameter resistive network for the thorax model was formulated by assuming that the ends of the cylinders are equipotential surfaces and by somewhat arbitrarily dividing the model volumes into 14 subvolumes. The cross-sectional area and length of each of these subvolumes were computed and the resistor analog selected by considering each of these subvolumes as a parallel combination of resistors. Resistor values were selected equal to the resistivities of the respective volumes multipled by the length of the volume. The number of resistors in parallel was then numerically equal to the cross-sectional area of the subvolume. The

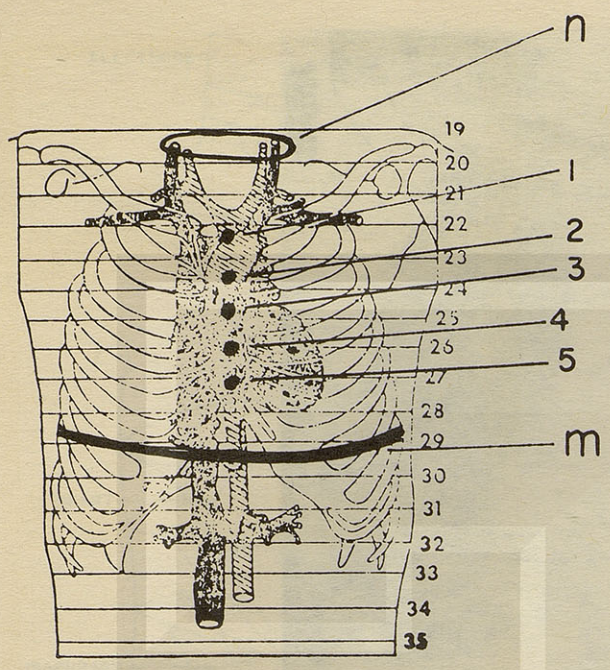

FIGURE 8

Surface electrode locations for waveforms in figure 7. Positions 1 to 5 anterior, over sternum.

entire network formulation is shown in figure 15a. The total resistance of this two-terminal network was computed to 46.3 ohms, which was comparable to an average measured impedance of approximately 36 ohms when the two band electrodes were used.

Considering the blood volume ejected from the heart during systole to be 140 cc. and the volume pumped to the lungs to be 70 cc., a second model and network were similarly developed to approximate the heart and lung volumes at the end of systole. The blood was assumed to be uniformly distributed to all lung subvolumes, increasing the subvolumes accordingly. An average 7% increase in the major vein- and artery-volume diameter was also assumed. This resulted in the network model shown in figure 15b. The total resistance of the second network was then 44.7 ohms. The 1.6-ohm decrease in computed resistance between the beginning and end of systole corresponded to an approximate 0.13-ohm decrease measured experimentally between the band electrodes.

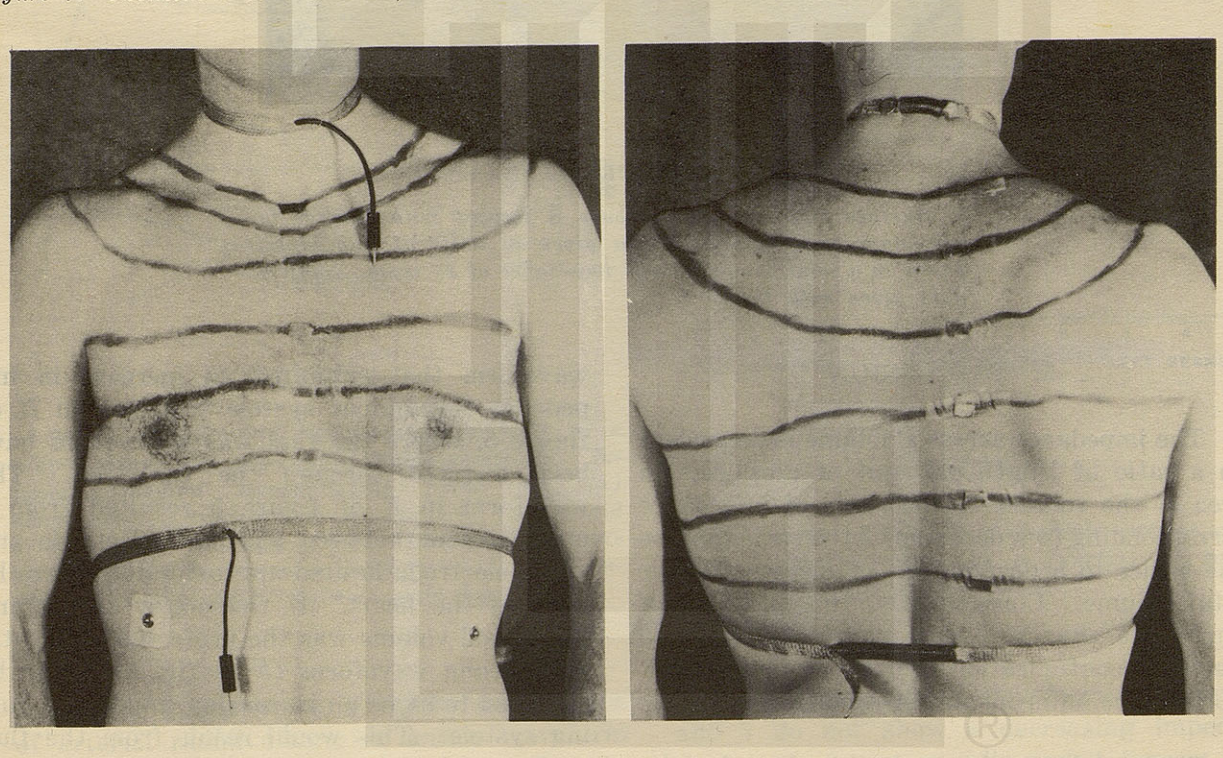

FIGURE 9

Surface equipotential contours for the band-electrode excitation.

Subject: 72.5 in., 168 lb., standing.

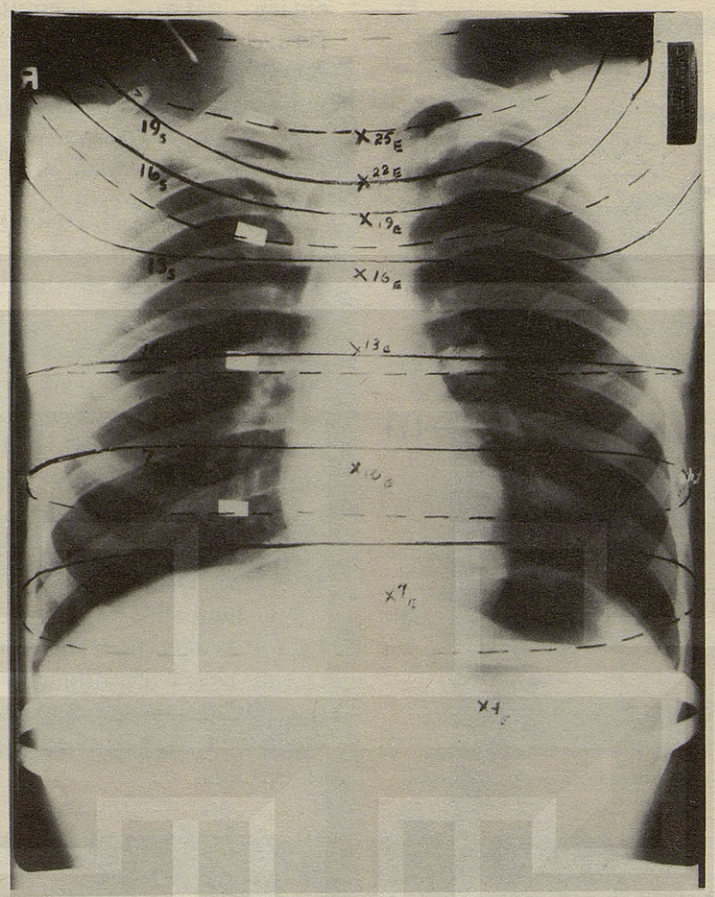

FIGURE 10

Surface equipotential contours S *located with respect to esophagus potentials* E. *Data given in units of impedance, based on a total band-electrode impedance of 33 ohms. Subject data given with figure 9.*

5. DISCUSSION

The impedance across a volume is dependent on a ratio of length per unit of cross-section area of the volume. A decrease of impedance corresponding to a decrease of the ratio may be due either to a decrease or an increase of the total volume. Consequently, the direction of impedance change during systole for a given electrode configuration is not a unique indication of the internal organ-volume change.

The waveforms obtained, while directing the current flux through various parts of the thorax, showed a dominant characteristic of decreasing impedance during systole. The only waveform that exhibited an increase in impedance throughout systole is shown in *H* of figure 5, where the flux was believed to have been directed through the ventricles. The waveform in *E* of figure 5 resulted from a measurement between the neck electrode and a cup electrode located approximately over the apex of the heart. If the major artery and vein blood volume was the preferred flux path, this second waveform (*F* in fig. 5) would be expected to show an increasing impedance during systole. This would result from the flux path continuing through the heart blood volume, with the resulting impedance increase as noted in *H* of figure 5. The opposite result was actually noted. This observed decrease of

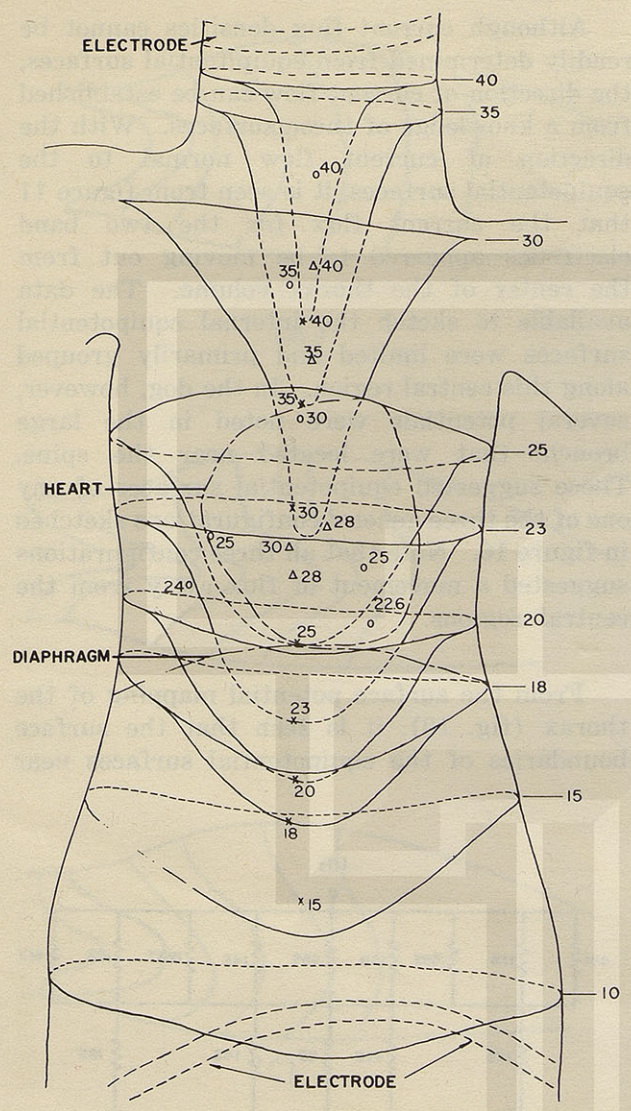

FIGURE 11

Sketch of estimated equipotential surfaces in a canine thorax for two-band-electrode excitation. Internal potential measurements noted as: (x) esophagus, (○) trachea and large bronchi, (△) carotid artery and heart. Ventrial view. Data given in units of impedance, based on a total band-electrode impedance of 50.1 ohms. Animal: male dog, 45 lb.

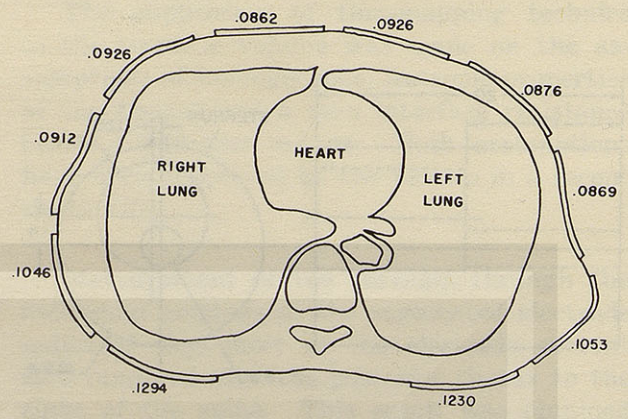

FIGURE 12

Percentage of total electrode current at each segment of the segmented band electrode, positioned at the third intercostal space.

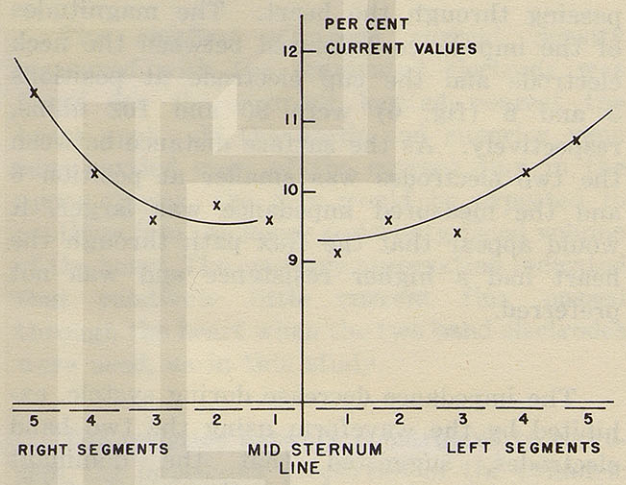

FIGURE 13

Percentage of total band-electrode current at the third intercostal space, as a function of position around the thorax perimeter.

impedance might be explained by an increase of arterial radial dimension and a waveform relatively insensitive to heart-volume changes. On the basis of results of other portions of the investigation, however, this possibility seems unlikely.

It is noted that all waveforms in figures 5 and 7 do not show a decreasing impedance during the entire systolic period (except *H* in fig. 5 and *G* in fig. 7). The increase at the end of systole, particularly in *E*, *F*, and *G* of figure 5 and *E* and *F* of figure 7, may possibly

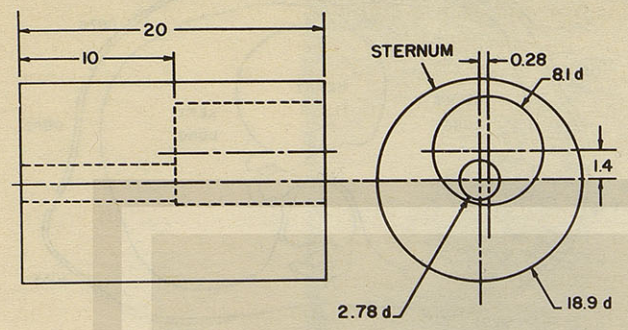

FIGURE 14

Simplified thorax model. Dimensions in centimeters.

be explained on the basis of either venous return from the lungs or a percentage of flux passing through the heart. The magnitudes of the impedance measured between the neck electrode and the cup electrode at positions 5 and 6 (fig. 6) were 90 and 102 ohms, respectively. As the surface distance between the two electrodes was smaller at position 6 and the measured impedance was larger, it would appear that the flux path through the heart had a higher resistance and was not preferred.

The impedance decrease during systole, exhibited by the waveform using the two band electrodes, suggested that the dominant characteristic observed was that blood of low resistivity moved into the thoracic regions and carried most of the current flux. The two possible regions in which this can occur are the pulmonary vascular bed and the primary arterial system. However, the waveform taken above the first rib with the three-electrode plethysmograph showed relatively little change in impedance (*B* in fig. 7). As the voltage drop between the neck electrode and position 1 was due to a constant current source, the effect of blood pulsations in the arteries above the rib cage appeared to produce minor contributions, if any, to the observed two-band waveform.

Although current flux densities cannot be readily determined from equipitential surfaces, the direction of current flow can be established from a knowledge of these surfaces. With the direction of current flow normal to the equipotential surfaces, it is seen from figure 11 that the current flux for the two band electrodes appeared to be moving out from the center of the thorax volume. The data available to sketch the internal equipotential surfaces were limited and primarily grouped along this central region. In the dog, however, several potentials were noted in the large bronchi that were located near the spine. These suggested equipotential surfaces of any one of the three general configurations sketched in figure 16. Note that all three configurations suggested a movement of flux away from the central regions.

From the surface potential mapping of the thorax (fig. 10), it is seen that the surface boundaries of the equipotential surfaces near

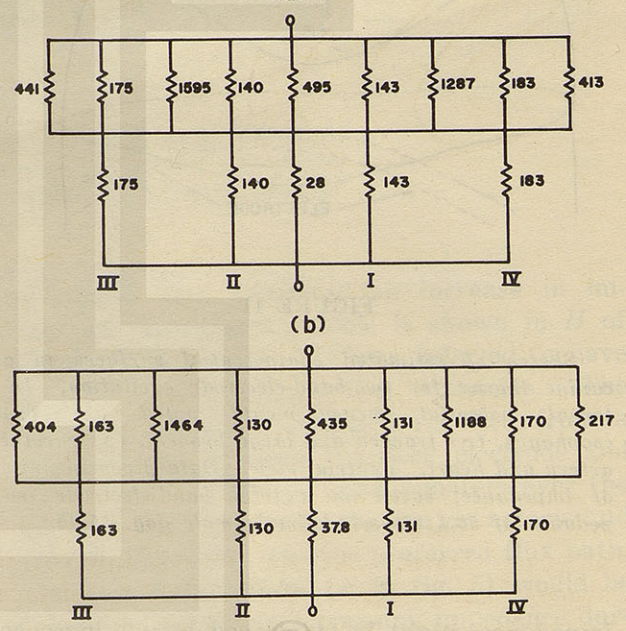

FIGURE 15

Approximate equivalent lumped parameter network of the thorax model, figure 14. The systole begins in (a)*; the diastole begins in* (b).

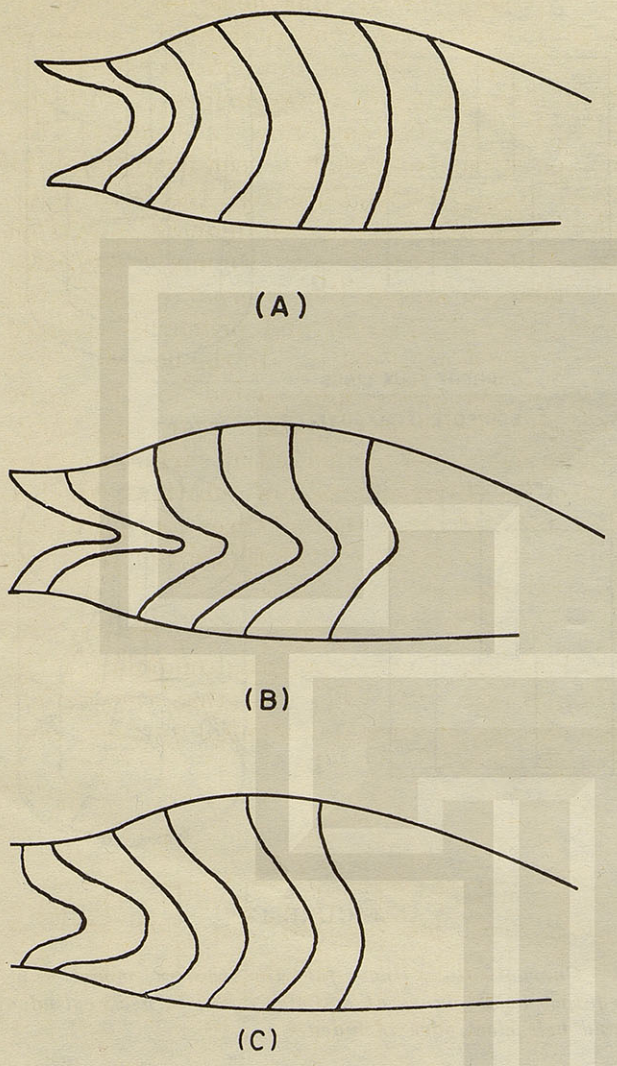

FIGURE 16

Estimated possible equipotential lines in the canine thorax for the two band electrodes, based on potential measurements located near the spine. Midsagittal view.

the base of the neck were more cephalad on the posterior thorax (dotted lines) than on the anterior thorax. At the fourth intercostal space, the posterior and anterior surface boundaries were nearly on a horizontal plane. This observation tended to suggest that the current flux moved from the neck region into the thorax toward the wall of the posterior chest and then vertically down through the lungs.

The application of flux-mapping technics to the thoracic volume was made on the assumptions of homogeneous, isotropic properties of the tissues and a zero interface resistance between adjacent organs. Both assumptions have been supported by the results in a recent study (2).

Measurement of the currents through the individual portions of the segmented electrode indicated that most of the electrode current flow occurred over the posterior thorax to the right of the spine. This result was obtained for locations of the segmented electrode at the midsection position indicated in figure 1 as well as at the level of the third intercostal space. With the largest electrode current flow occurring to the right of the spine and with the descending aorta located to the left of the spine (fig. 12), the lungs again appeared to provide the principal flux path.

The smallest electrode current density measured with the segmented electrode was found for the segment located nearest the heart apex. If the aorta and superior vena cava carried most of the current flux in the upper thorax, the flux would be expected to continue into the lower resistivity blood volume of the heart. The contrary observation indicated that relatively little current flux passed through the heart when the two band electrodes were used, as in this study.

The resistive network constructed to represent the impedance properties of the cylindric model of the thorax resulted in a computed impedance of 46.3 ohms. This value compared reasonably well with the average measured value of 36 ohms, considering the character of the thorax model, and the assumed equipotential plane excitation surfaces relative to the current source applied to the subject's thorax. The change in the model impedance during systole corresponded with observation and further justified use of the model, even though the magnitudes of the changes were different.

The estimated equipotential surfaces within the cylindric model were found to be convex

cephalad when both ends of the cylinder were considered as equipotentials (fig. 17a). When a neck cylinder was added to the model, however, and the model was excited by electrodes similar to the electrode placements on the subjects, the equipotential surfaces were estimated to be concave cephalad (fig. 17b). These latter concave surfaces corresponded with the results obtained for both human and animal subjects, on the basis of potential measurements, thus tending to validate both procedures.

The inner cylinder of the model representing the blood volume of the primary arterial-venous system of the upper thorax had a computed resistance value of 495 ohms while the resistance of the parallel lung volume was computed to be approximately 32 ohms. This indicated that most of the current flux would tend to travel through the model lungs in this region. From dimensions of the aorta of a dog and the known resistivity of blood, it was found that a 10-cm. length of the aorta had a total impedance of 3,100 ohms. When this total value was compared with the impedance of the animal thorax between the two standard band electrodes, the conclusion was again in agreement with the results found for the model; that is, the impedance of the arterial-venous system was much greater than the total thoracic impedance and was not a preferred current flux path.

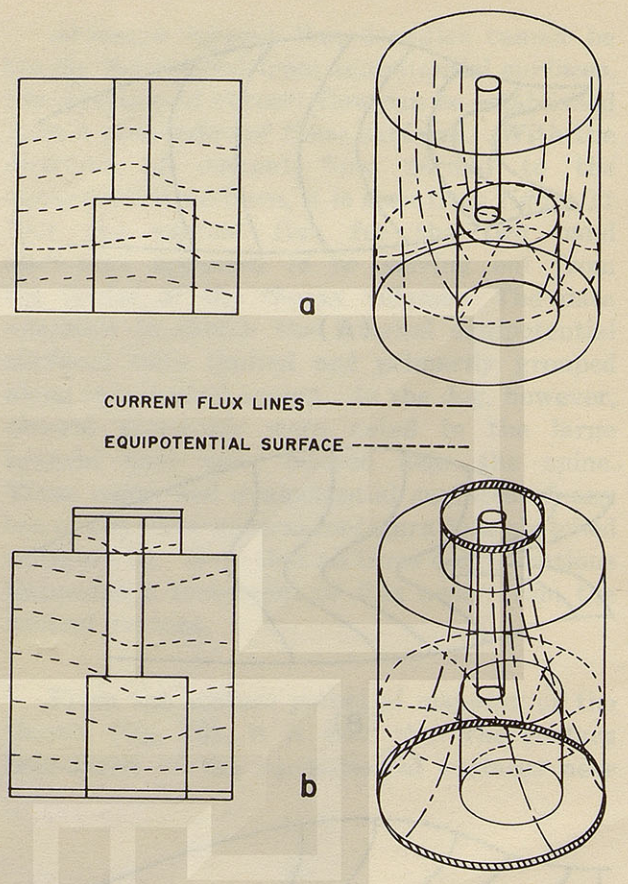

FIGURE 17

Current flux lines for the thorax model: **a**, *equipotential planes at cylinder ends;* **b**, *neck cylinder and belt electrodes included.*

REFERENCES

1. Kinnen, E., W. Kubicek, and R. Patterson. Thoracic cage impedance measurements: Impedance plethysmographic determination of cardiac output (a comparative study). SAM-TDR-64-15, Mar. 1964.

2. Kinnen, E., W. Kubicek, P. Hill, and G. Turton. Thoracic cage impedance measurements: Tissue resistivity in vivo and transthoracic impedance at 100 kc. SAM-TDR-64-5, Mar. 1964.

SCHOOL OF AEROSPACE MEDICINE
AEROSPACE MEDICAL DIVISION (AFSC)
BROOKS AFB TEX

POSTAGE AND FEES PAID

UNITED STATES AIR FORCE
OFFICIAL BUSINESS
RETURN REQUESTED

THIRD CLASS MAIL

LT COL H. GRADY WISE

1 OF 2

SAM MAIL BOX 4475

AFPS SA JUN 64 2230